# A thermodynamic chemical reaction network drove autocatalytic prebiotic peptides formation

Peng Bao [a,b,c,*], Yu-Qin He [a,b,c], Guo-Xiang Li [d], Hui-En Zhang [e], Ke-Qing Xiao [f]

[a] *Key Lab of Urban Environment and Health, Institute of Urban Environment, Chinese Academy of Sciences, Xiamen 361021, PR China*
[b] *Ningbo Urban Environment Observation and Station, Chinese Academy of Sciences, Ningbo 315800, PR China*
[c] *University of Chinese Academy of Sciences, Beijing 100049, PR China*
[d] *Center for Applied Geosciences (ZAG), Eberhard Karls University Tuebingen, Sigwartstrasse 10, Tuebingen 72076, Germany*
[e] *College of Biological and Environmental Sciences, Zhejiang Wanli University, Ningbo 315100, PR China*
[f] *School of Earth and Environment, University of Leeds, Leeds LS2 9JT, UK*

## Abstract

The chemical reaction networks (CRNs), which led to the transition on early Earth from geochemistry to biochemistry remain unknown. We show that the simplest substances—bicarbonate, sulfite/sulfate, and ammonium—were converted to peptides in one geological setting from Sammox (sulfite/sulfate reduction coupled to anaerobic ammonium oxidation)-driven CRNs under mild hydrothermal conditions. Peptides comprise 15 proteinogenic amino acids, endowed Sammox-driven CRNs with autocatalysis. The peptides exhibit both forward and reverse catalysis, with the opposite catalytic impact in sulfite- and sulfate-fueled Sammox-driven CRNs, respectively, at both a variable temperature range and a fixed temperature, resulting in seesaw-like catalytic properties. The variation of substrates concentration and temperature, can influence the redox property of the system, may disrupt the redox homeostasis of Sammox-driven CRNs, therefore, the catalytic orientation of peptides changed due to the stimulation, to maintain system redox homeostasis. The seesaw-like catalytic characteristics of peptides is critical to achieving the sustainability and evolution of Sammox-driven CRNs by preferentially destroy non-functional peptides and preserve peptides with high substrate specificities and/or novel functions. Moreover, the peptides generated from sulfite-fueled Sammox-driven CRNs could catalyze both sulfite-fueled Sammox, and Anammox (nitrite reduction coupling with anaerobic ammonium oxidation) reactions. We propose that Sammox-driven CRNs were critical in the creation of life and that Sammox and Anammox are primordial energy conservation traits.
© 2022 The Author(s). Published by Elsevier Ltd. This is an open access article under the CC BY license (http://creativecommons.org/licenses/by/4.0/).

## 1. INTRODUCTION

The chemistry of life can be thought of as autocatalytic organized chemical reaction networks (CRNs), which involve coupling transformation of six key elements—carbon (C), hydrogen (H), oxygen (O), nitrogen (N), sulfur (S), and phosphorous (P) (Kauffman 1986; Falkowski et al., 2008; Hordijk et al., 2018). We speculate that there might have been a thermodynamic chemical reaction network, which involved C, H, O, N, and S, initiated by exergonic redox reactions, resulting in the development of the proto-metabolic networks (PMNs) in primordial phosphorous-deficient circumstances. The importance of N and S geochemical transformations in the origin of life has been majorly overlooked. A recent study has demonstrated the vital role of sulfur reduction and anaerobic

ammonium oxidation in the origin of life (Li et al., 2020a). Phylogenetic distribution and functional grouping of sulfite reductase clusters show that a sulfite reductase, with a coupled siroheme-[Fe$_4$-S$_4$] cluster, was most likely present in the last universal common ancestor (LUCA) (Crane et al., 1995; Molitor et al., 1998; Dhillon et al., 2005). Nitrite reduction coupled with anaerobic ammonium oxidation (Anammox) might be an ancient metabolism because Anammox organisms could be the first nascent bacterial species (Brochier and Philippe, 2002; van Niftrik and Jetten, 2012), and might be the evolutionary kinds between the three domains of life (Reynaud and Devos, 2011).

Sulfite was richly produced on early Earth from volcanic and hydrothermal sulfur dioxide (Ono et al., 2003; Canfield et al., 2006; Anbar 2008; Falkowski et al., 2008; Moore et al., 2017). Most of the nitrogen species in hydrothermal fluids released from the mantle of the reduced young Earth into the early oceans might have comprised mostly ammonium (Li and Keppler, 2014; Mikhail and Sverjensky, 2014). As a result, spontaneous redox reaction transfers for energy generation and organic molecule synthesis occurred when the prebiotically plausible sulfurous species and ammonium in early Earth hydrothermal environments encountered carbon dioxide. We hypothesize that thermodynamically feasible CRNs containing $HCO_3^-$, $H_2O$, $NH_4^+$, $SO_3^{2-}/SO_4^{2-}$, and $HS^-$ (Fig. 1) (Balcerowiak 1985; Amend and Shock, 2001; Fdz-Polanco et al., 2001; Amend et al., 2003; Schrum et al., 2009; Wang et al., 2013; He et al., 2019; Li et al., 2020b; Wu et al., 2020), might produce PMNs. In this CRNs, sulfur reduction, nitrite reduction coupled with anaerobic ammonium oxidation are all included (Fig. 1; Eqs. (1), (2), and (3)). The reducing power from the reaction (Sammox) could drive the CRNs (Li et al., 2020a).

The reactions in Sammox-driven CRNs are nonlinear and connected in intricate ways. As a result, we only offer the reaction equation up to the formamide, which acts as a chemical precursor for the production of metabolic and genetic apparatus intermediate (Saladino et al., 2012), (Fig. 1; Eq. (11)). The Sammox-driven CRNs were nonequilibrium thermodynamic CRNs, which provide energy and material for the development of PMNs. Peptides are the best-known biocatalysts in the cell and the molecular hubs in the origin of life, therefore the PMNs should have at least started with carbon fixation, reductive amination, and continued until peptides production (Frenkel-Pinter et al., 2020). As a result, prebiotic CRNs, which resulted in the origin of life should have contributed to the autocatalysis of the PMNs. In this study, we demonstrate evidence of peptides production, and the origin of autocatalysis in Sammox-driven CRNs comprising $HCO_3^-$, $NH_4^+$, $SO_3^{2-}/SO_4^{2-}$ under mild hydrothermal circumstances providing a novel option of the earliest origin of life.

## 2. MATERIAL AND METHODS

### 2.1. Chemicals and reagents

All chemical reagents and organic solvents were of analytical grade. Detailed information is as follows: ammonium chloride (>99.5%, CAS number: 12125–02–9), ammonium formate (>97%, CAS number: 540–69–2) were acquired from Sigma–Aldrich, USA. Sodium sulfate (>99.9%, CAS number: 7757–82–6), sodium sulfide nonahydrate (>98%, CAS number: 1313–84–4), acetonitrile (>99.9%, CAS number: 75–05–8), methanesulfonic acid (>99.5%, CAS number: 75–75–2) were purchased from Aladdin, USA. Sodium sulfite (>98.5%, CAS number: 7757–83–7), oxalacetic acid (>98%, CAS number: 328–42–7), α-Ketoglutaric acid, disodium salt, dehydrate (>99%, CAS number: 305–72–6) were purchased from Acros Organics, Belgium. Pyruvic acid sodium (>98%, CAS number: 113–24–6) was purchased from Amresco, USA. Methanol (>99.9%, CAS number: 67–56–1) was obtained from Tedia, USA. Sodium acetate anhydrate (>99%, CAS number: 127–09–3) was purchased from Sangon Biotech, China. Sodium bicarbonate (>99%, CAS number: 144–55–8) was purchased from Macklin, China. Peptide digest assay standard (Pierce$^{TM}$ Quantitative Colorimetric Peptide Assay, Thermo Scientific, USA) was

$$6NH_4^+ + 3SO_3^{2-} \rightarrow 3N_2 + 3H_2S + 9H_2O \quad \cdots \cdots \text{(Equation 1) (Amend and Shock, 2001)}$$

$$4NH_4^+ + 3SO_4^{2-} \rightarrow 4NO_2^- + 3S^{2-} + 4H_2O + 8H^+ \quad \cdots \text{(Equation 2) (Fdz-Polanco et al., 2001; Amend et al., 2003; Schrum et al., 2009)}$$

$$2NO_2^- + 2NH_4^+ \rightarrow 2N_2 + 4H_2O \quad \cdots \cdots \text{(Equation 3) (Fdz-Polanco et al., 2001; Amend et al., 2003; Schrum et al., 2009)}$$

$$2NO_2^- + 3S^{2-} + 8H^+ \rightarrow 3S^o + N_2 + 4H_2O \quad \cdots \cdots \text{(Equation 4) (Fdz-Polanco et al., 2001; Amend et al., 2003; Schrum et al., 2009)}$$

$$HS^- + (x-1)H_2O + OH^- + xCO_2 \rightarrow SOx^{2-} + xHCOOH \quad \cdots \cdots \text{(Equation 5; x=3 or 4) (He et al., 2019)}$$

$$HS^- + H_2O \xrightarrow{OH^-} SOx^{2-} + H_2 \quad \cdots \cdots \text{(Equation 6; x=3 or 4) (Wang et al., 2013)}$$

$$HCOOH + NaHCO_3 \rightarrow HCOONa + H_2O + CO_2 \quad \cdots \cdots \text{(Equation 7)}$$

$$2HCOONa \rightarrow Na_2CO_3 + H_2 + CO \quad \cdots \cdots \text{(Equation 8) (Balcerowiak 1985; Li et al., 2020b)}$$

$$2HCOONa \rightarrow Na_2C_2O_4 + H_2 \quad \cdots \cdots \text{(Equation 9) (Balcerowiak 1985; Li et al., 2020b)}$$

$$HCOOH + NH_3 \rightarrow HCOONH_4 \quad \cdots \cdots \text{(Equation 10) (Wu et al., 2020)}$$

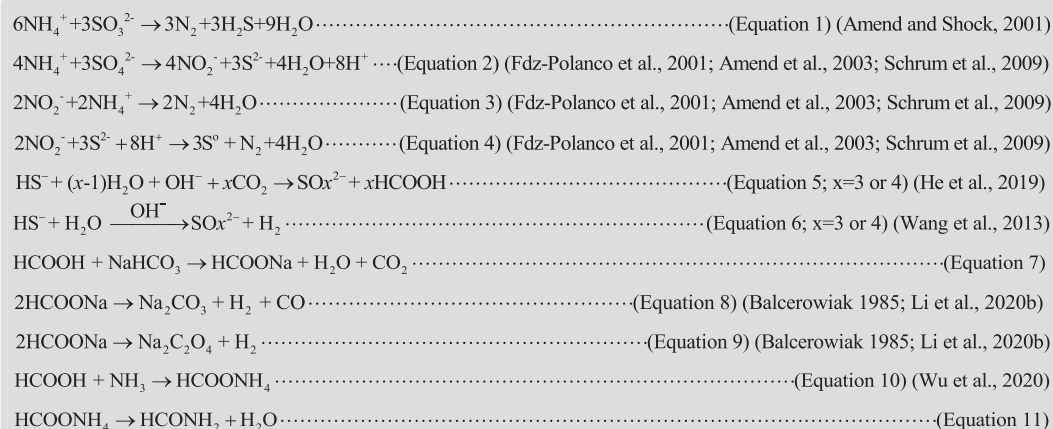$$HCOONH_4 \rightarrow HCONH_2 + H_2O \quad \cdots \cdots \text{(Equation 11)}$$

Fig. 1. Proposed reactions for the Sammox-driven CRNs. Sammox: equations 1, 2, 3, 4. $CO_2$ reduction: equations 6, 7, 8, 9. N activation: equations 10, 11.

as standard for quantitative analysis of peptides. All reagents were utilized without further purification unless otherwise noted. Ultrapure water was prepared employing the Millipore purification system (Billerica, MA, USA).

## 2.2. General procedure for Sammox reactions

A total of 100 mL ultrapure water was introduced into 120 mL serum bottles and sealed with butyl rubber stoppers and aluminum crimp caps. The solution in the serum bottles was autoclaved and cooled at 25 °C after being flushed with helium (He) gas (purity = 99.999%). Additional sulfite, sulfate, ammonium, and bicarbonate were introduced into the serum bottles as the "Sammox reaction system." The above-mentioned ingredients were aseptically introduced to the serum bottles as follows: sodium sulfite, and sulfate (1 mL, 3 mM final concentration), ammonium solution (0.5 mL, 6 mM final concentration for sulfite group; 0.5 mL, 8 mM final concentration for sulfate group), bicarbonate solution (1 mL, 20 mM final concentration). The initial pH value is roughly 8.2. The reaction systems were heated at 100 °C in a water bath in the dark for 24 h, maintained at 70 °C in the dark for 24 h, and removed from the water bath, and left to cool to room temperature before the investigation was conducted.

This investigation was performed employing the following series of experiments:

(i) 3 mM sulfite/sulfate/sulfide + 6/8 mM $NH_4Cl$ + 20 mM $HCO_3^-$,
(ii) 3 mM sulfite/sulfate/sulfide + 20 mM $HCO_3^-$,
(iii) 6/8 mM $NH_4Cl$ + 20 mM $HCO_3^-$,
(iv) ultrapure water

## 2.3. General procedure for the reductive amination of keto acids with $HCOONH_4$

To further confirm the feasibility of the reductive amination of keto acids with $HCOONH_4$, We employed $HCOONH_4$, pyruvic acid, oxaloacetate, and α-ketoglutarate (3.0 mM final concentration), as substrates in hydrothermal reaction systems. Serum bottles were heated at 70 °C in a water bath in the dark for 48 h, maintained in the dark, and left to cool to room temperature before investigation. This investigation was conducted employing the following series of experiments:

(i) 3.0 mM $HCOONH_4$ + 3.0 mM pyruvic acid.
(ii) 3.0 mM $HCOONH_4$ + 3.0 mM oxaloacetate.
(iii) 3.0 mM $HCOONH_4$ + 3.0 mM α-ketoglutarate.

## 2.4. Autocatalysis of the Sammox-driven CRNs

We designed as simple as possible experiments to confirm whether the Sammox-driven CRNs already have autocatalysis. The experimental procedure was conducted in two rounds. In the first round procedure, serum bottles containing Sammox reaction solution were heated at 100 °C in a water bath in the dark for 24 h, maintained at 70 °C in the dark for another 24 h, and left to cool to room temperature. One milliliter of the first round Sammox reaction solutions (sulfite/sulfate-fueled Sammox) was extracted, and injected into newly prepared Sammox reaction solution (the second round) (sulfite/sulfate-fueled Sammox) as a potential catalyst, respectively. The second round Sammox reaction was executed at two temperature settings 100 °C 24 h–70 °C and 45 °C 48 h and allowed to cool to room temperature before sampling. See Fig. 5 a for a detailed description of the experimental design.

## 2.5. Peptides facilitate sulfite-fueled Sammox and Anammox reactions

Serum bottles containing sulfite-fueled Sammox reaction solution were heated at 100 °C in a water bath in the dark for 24 h, maintained at 70 °C in the dark for another 24 h, and left to cool to room temperature. One milliliter of the products was extracted and injected into newly prepared sulfite-fueled Sammox reaction solution (3.0 mM sulfite; 6.0 mM ammonium) and Anammox reaction solution (6.0 mM nitrite; 6.0 mM ammonium), respectively, as a potential catalyst. The reactions were all executed at 100 °C, 24 h–70 °C, 24 h, and left to cool to room temperature before sampling for analysis of sulfite, sulfate, thiosulfate, nitrite, and ammonium.

## 2.6. Sampling analytical methods

### 2.6.1. High-performance liquid chromatography quantitative analysis of peptides

Solution samples were freeze-dried and diluted with ultrapure water to 1.0 mL. The High-performance liquid chromatography system (Agilent LC-1260, USA) comprised a Phenomenex Luna CN 5u column, which is a non-porous analytical column, packed with 5 μm particles (250 mm × 4.6 mm inner diameter, Phenomenex Inc, USA). Mobile phase A comprised 0.05 M sodium acetate, while solvent B was 20% methanol–60% acetonitrile–20% ultrapure water. The samples were investigated utilizing isocratic elution circumstances with an eluent A/B (80:20) for 15 min. The flow rates of the mobile phase and the column temperature were set at 1 mL min$^{-1}$ and 35 °C, respectively. The detection wave was UV-214 nm by a diode array detector. Peptides were determined by comparing the retention times against commercially standard peptides. Peptide standard solutions were prepared with concentration gradients of 25, 50, 75, 100, 250 and 500 ug mL$^{-1}$.

### 2.6.2. High-performance liquid chromatography quantitative analysis of thiosulfate

The concentration of thiosulfate was determined employing an Agilent 1260 Infinity HPLC system, equipped with a quaternary pump (Agilent, USA). Thiosulfate was separated with a Zorbax SB-C18 column (150 × 4.6 mm, 5 μm) and detected utilizing a DAD detector at 215 nm. All analyses were performed at 40 °C with a flow rate of 1 mL min$^{-1}$. $Na_2HPO_4$ was employed as the solvent. The pH of the solvent was modified with 1.0 M HCl to 8.5.

Samples were filtered with 0.45 μm Cosmonice Filters (Millipore, Tokyo, Japan) and immediately injected into the HPLC system (Li et al., 2020a).

### 2.6.3. Nano LC-MS/MS identification of peptides and amino acids

Solution samples were freeze-dried and diluted with ultrapure water to 1.0 mL. The sample solution was reduced using 10 mM DTT at 56 °C for 1 h and alkylated with 20 mM IAA at room temperature, in dark for 1 h. Thereafter, the extracted peptides were lyophilized to almost dryness and resuspended in 2–20 μL of 0.1% formic acid before LC-MS/MS investigation. LC-MS/MS investigation was executed on the UltiMate 3000 system (Thermo Fisher Scientific, USA) coupled to a Q Exactive™ Hybrid Quadrupole-Orbitrap™ Mass Spectrometer (Thermo Fisher Scientific, USA). The chromatographic separation of peptides was obtained using a nanocolumn—a 150 μm × 15 cm column—made in-house and packed with the reversed-phase ReproSil-Pur C18-AQ resin (1.9 μm, 100 A, Dr. Maisch GmbH, Germany). A binary mobile phase and gradient were employed at a flow rate of 600 mL min$^{-1}$, directed into the mass spectrometer. Mobile phase A was 0.1% formic acid in the water, and mobile phase B was 0.1% formic acid in acetonitrile. LC linear gradient: from 6%–9% B for 5 min, from 9%–50% B for 45 min, from 50%–95% B for 2 min, and from 95%–95% B for 4 min. The injection volume was 5 μL. MS parameters were set as follows: resolution at 70,000; AGC target at 3e6; maximum IT at 60 ms; the number of scan ranges at 1; scan range at 300 to 1,400 m/z; and spectrum data type was set to profile. MS/MS parameters were set as follows: resolution was set at 17,500; AGC target at 5e4; maximum IT at 80 ms; loop count at 20; MSX count at 1; TopN at 20; isolation window at 3 m/z; isolation offset at 0.0 m/z; scan range at 200 to 2,000 m/z; fixed first mass at 100 m/z; stepped NCE at 27; spectrum data type at profile; intensity threshold at 3.1e4; and dynamic exclusion at 15 s. The raw MS files were investigated and searched against target protein databases, based on the species of the samples utilizing Peaks studio and MaxQuant (1.6.2.10), combined with manual comparison in the UniProt and NCBI databases. The parameters were set as follows: protein modifications were carbamidomethylation (C) (fixed), oxidation (M) (variable), and acetylation (N-term) (variable); enzyme was set to unspecific; the maximum missed cleavages were set to 2; the precursor ion mass tolerance was set to 20 ppm, and MS/MS tolerance was 20 ppm. Only peptides determined with high confidence were chosen for downstream protein determination investigation.

For the analysis of amino acids content, solution samples were freeze-dried, and diluted with ultrapure water to 1.0 mL, followed by acid hydrolysis. A total of 10 μL acid hydrolysate was mixed with 30 μL acetonitrile, vortexed for 1 min, and centrifuged for 5 min at 13,200 r min$^{-1}$ at 4 °C. Thereafter, 10 μL of supernatant was introduced to 10 μL water and vortexed for 1 min. Subsequently, 10 μL of the mixture was introduced to 70 μL of borate buffer (from AccQTag kit) and vortexed for 1 min. A total of 20 μL of AccQ Tag reagent (from AccQTag kit) was introduced to the sample, vortexed for 1 min, and the sample was left to stand at ambient temperature for 1 min. Finally, the solution was heated for 10 min at 55 °C, and centrifuged for 2 min at 13,200 r min$^{-1}$ and 4 °C.

Multiple reaction monitoring investigations were done by utilizing a Xevo TQ-S mass spectrometer. All experiments were conducted in positive electrospray ionization (ESI+) mode. The ion source temperature and capillary voltage were kept constant and set to 150 °C and 2 kV, respectively. The cone gas flow rate was 150 L h$^{-1}$ and the desolvation temperature was 600 °C. The desolvation gas flow was 1,000 bar. The system was regulated with the analysis software.

### 2.6.4. Ion chromatography quantitative analysis of sulfite, sulfate, nitrite, and ammonium

To determine sulfite, sulfate, and nitrite, 1.0 mL of the sample was filtered (0.22 μm) to remove particulates that could interfere with ion chromatography. The ion chromatography system comprised an ICS-5000$^+$ SP pump (Thermo Fisher Scientific Inc. Sunnyvale, CA, USA), a column oven ICS-5000$^+$ DC, an electrochemical detector DC-5. The ion chromatography column system utilized was a Dionex Ionpac AS11-HC column. The operating condition was with an eluent of 30 mM KOH at a flow rate of 1.0 mL min$^{-1}$. For the determination of ammonium, the ion chromatography column system employed was a Dionex IonpacTM CS 12A column. The operating condition was with an eluent of 20 mM sulphonethane at a flow rate of 1.0 mL min$^{-1}$.

## 3. RESULTS

### 3.1. Peptides formation in Sammox-driven CRNs

Determination of the likely end product of Sammox-driven CRNs was the primary goal of this study. We detected formate as initial product of Sammox-driven CRNs, and peptides as the end products of sulfite/sulfate-fueled CRNs in experiments described in part 2.2 (Fig. 2 a, b). However, no peptides or very low concentrations of peptides were produced in sulfide-fueled CRNs (Fig. 2 c), which may require a higher reaction temperature and/or accelerator. In experiments described in part 2.3, ammonium formate reacted with pyruvate to produce serine, glycine, aspartate, glutamate, alanine, valine, and leucine (Table 1; Fig. S1). Ammonium formate reacted with oxaloacetate to produce serine, glycine, aspartate, glutamate, asparagine, threonine, tyrosine, leucine, and a high level of alanine up to 268 μM (Table 1; Fig. S2). Ammonium formate reacted with α-ketoglutarate to produce serine, glycine, aspartate, alanine, threonine, arginine, proline, lysine, valine, leucine, and a high level of glutamate up to 46 μM (Table 1; Fig. S3). We have not detected free proteinogenic amino acids in Sammox-driven CRNs (data not shown).

Fig. 3 indicates a chromatogram of peptides generated from Sammox-driven CRNs (Fig. S4). Fig. 3 b indicates the peak of standard peptides that appeared in similar retention times of target peptides in the sample, verifying
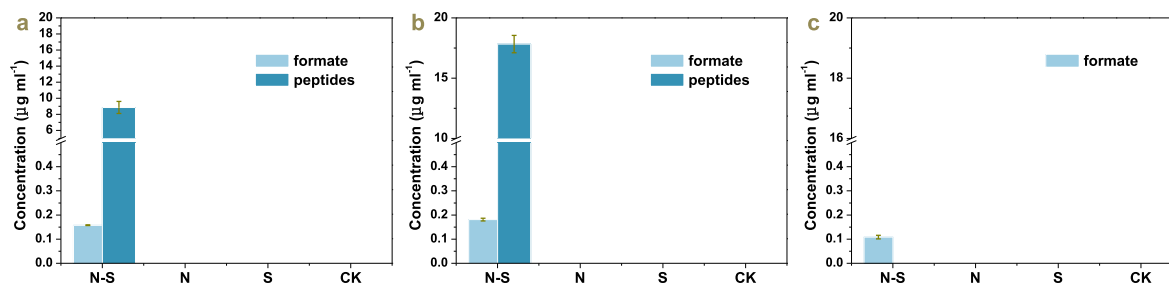
Fig. 2. Organic compounds developed from Sammox-driven prebiotic CRNs with bicarbonate as the sole carbon source under mild hydrothermal conditions. Treatments were as follows (a, sulfite-fueled CRNs; b, sulfate-fueled CRNs; c, sulfide-fueled CRNs) from left to right, N-S: ammonium + sulfurous species, N: ammonium, S: sulfurous species, CK. The bar chart indicates the output of formate and peptides in each treatment group. Error bars represent standard deviations of three replicates.

the feasibility of the standard peptides. Table 2 demonstrates selected identified peptides produced from Sammox-driven CRNs (Fig. S5, S6), and Fig. 4 representative MS/MS spectra of identified peptides produced from Sammox-driven CRNs. Peptides comprised 15 proteinogenic amino acids, including alanine, glycine, valine, histidine, leucine, serine, aspartate, asparagine, lysine, glutamate, tyrosine, threonine, proline, arginine, and cysteine (Table 1; Fig. S7 and S8). Ornithine was also detected in sulfite/sulfate-fueled CRNs and ammonium formate with α-ketoglutarate groups (Table 1). Extracted ion chromatogram of amino acids standards is shown in Fig. S9.

### 3.2. The emergence of autocatalysis in Sammox-driven CRNs

In experiments described in part 2.4, we established series of investigations to confirm whether the Sammox-driven CRNs already has autocatalysis, by using Sammox-driven CRNs products to self-catalyze Sammox-driven CRNs. A 1.0 mL Sammox reaction solution (the first round sulfite/sulfate-fueled Sammox) was injected into freshly prepared Sammox reaction solution (the second round sulfite/sulfate-fueled Sammox) as the potential catalyst (Fig. 5 a). First, we examined the potential catalysis of products

to Sammox-driven CRNs in a variable temperature range, 100 °C 24 h–70 °C 24 h. Then, we investigated the potential catalysis of products to Sammox-driven CRNs in a selected biologically significant temperature, 45 °C 48 h. Surprisingly, products that were generated from sulfite-fueled Sammox reaction (100 °C–70 °C) could facilitate peptides generation in sulfite-fueled Sammox-driven CRNs at 100 °C–70 °C, and in sulfate-fueled Sammox-driven CRNs at 45 °C; but inhibited peptides generation in sulfate-fueled Sammox-driven CRNs at 100 °C–70 °C, and in sulfite-fueled Sammox-driven CRNs at 45 °C (Fig. 5 a; Figs. 6, 7, S10, and S11). Products that were generated from sulfate-fueled Sammox reaction (100 °C–70 °C), could inhibit peptides generation in sulfite-fueled Sammox-driven CRNs at 100 °C–70 °C, and in sulfate-fueled Sammox-driven CRNs at 45 °C; but facilitate peptides generation in sulfate-fueled Sammox-driven CRNs at 100 °C–70 °C, and in sulfite-fueled Sammox-driven CRNs at 45 °C (Fig. 5 a; Figs. 6, 7, S10, and S11). As we have demonstrated that there are no free proteinogenic amino acids or the content is very low in Sammox-driven CRNs. The Sammox-driven CRNs-generated peptides are most likely to be the catalysts, which could be complex enough to facilitate the emergence of reflexive autocatalysis, making

### Table 1
Proteinogenic amino acids abundance in peptides and non-proteinogenic amino acids in Sammox-driven CRNs. Amino acids abundance in reactions of ammonium formate (AF) with α-keto acids. The associated errors are standard deviations of three replicates. ND, not detected.

| Amino acids | Concentrations (μM) | | | | |
| --- | --- | --- | --- | --- | --- |
| | Sulfite-fueled CRNs | Sulfate-fueled CRNs | AF + pyruvate | AF + oxaloacetate | AF + α-ketoglutarate |
| Serine | 4.96 ± 1.35 | 3.54 ± 0.65 | 3.20 ± 1.17 | 1.92 ± 0.90 | 3.26 ± 1.67 |
| Glycine | 3.25 ± 0.38 | 2.92 ± 0.73 | 3.08 ± 1.02 | 2.76 ± 1.42 | 5.25 ± 2.32 |
| Aspartate | 2.42 ± 0.39 | 0.97 ± 0.46 | 1.03 ± 0.22 | 0.77 ± 0.33 | 1.79 ± 0.63 |
| Glutamate | 1.81 ± 0.26 | 10.14 ± 4.17 | 1.48 ± 0.24 | 3.73 ± 1.12 | 46.93 ± 10.92 |
| Alanine | 2.66 ± 0.38 | 1.81 ± 0.52 | 1.83 ± 0.18 | 268.25 ± 35.69 | 2.02 ± 0.21 |
| Asparagine | 0.36 ± 0.22 | ND | ND | 0.11 ± 0.01 | ND |
| Threonine | 0.77 ± 0.28 | 0.73 ± 0.24 | ND | 1.12 ± 0.89 | 0.99 ± 0.29 |
| Arginine | 0.40 ± 0.15 | 0.55 ± 0.03 | ND | ND | 0.79 ± 0.44 |
| Histidine | 0.53 ± 0.14 | 0.64 ± 0.14 | ND | ND | ND |
| Proline | 0.57 ± 0.05 | 0.59 ± 0.09 | ND | ND | 0.68 ± 0.24 |
| Lysine | 0.44 ± 0.05 | 0.50 ± 0.21 | ND | ND | 0.88 ± 0.31 |
| Tyrosine | 0.53 ± 0.34 | ND | ND | 0.32 ± 0.13 | ND |
| Valine | 0.49 ± 0.07 | 0.53 ± 0.14 | 0.72 ± 0.19 | ND | 0.82 ± 0.32 |
| Leucine | 0.67 ± 0.09 | 0.74 ± 0.18 | 0.97 ± 0.19 | 0.78 ± 0.28 | 1.20 ± 0.55 |
| Cysteine | 0.36 ± 0.13 | 0.31 ± 0.27 | ND | ND | ND |
| Ornithine | 0.55 ± 0.16 | 0.64 ± 0.27 | ND | ND | 0.38 ± 0.18 |
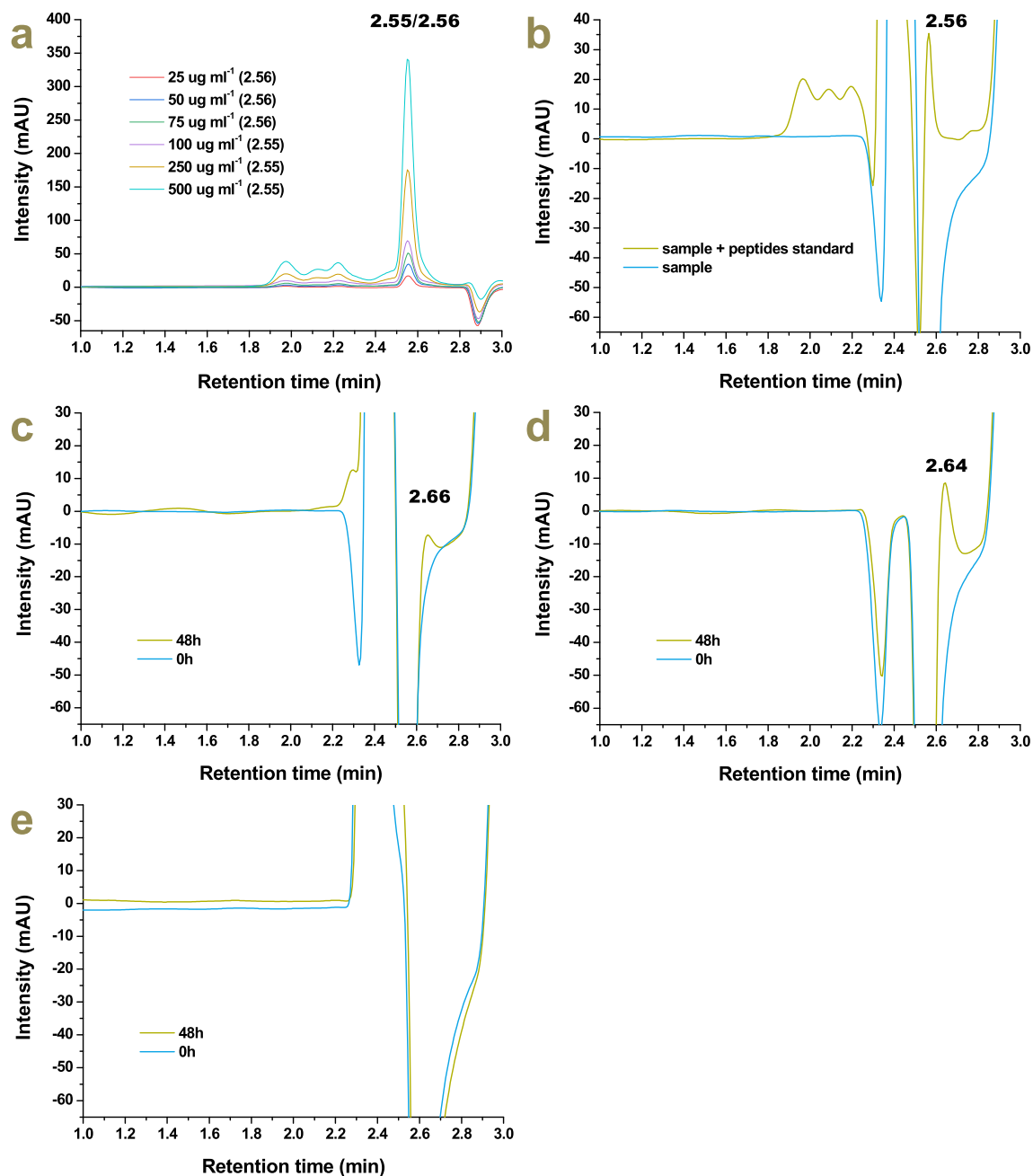
Fig. 3. Chromatogram of peptides developed from Sammox-driven CRNs, with bicarbonate as the sole carbon source, under mild hydrothermal conditions. The detection was performed at 214 nm. A, peptides standards (the retention time for each concentration is demonstrated accordingly in brackets); b, a 0.4 ml of 0 h sample of sulfite-fueled Sammox-driven CRNs added into 0.3 ml peptides standards (500 µg mL$^{-1}$); c, sulfite-fueled Sammox-driven prebiotic CRNs; d, sulfate-fueled Sammox-driven prebiotic CRNs; e, sulfide-fueled Sammox-driven prebiotic CRNs. The number illustrates the retention time of peptides peaks.

Sammox-driven CRNs autocatalytic (Figs. 5 b, 8). The peptides might have the reverse catalytic capacity that led to the inhibition phenomenon of peptides production in the corresponding treatment groups. It seemed that peptides presented bidirectional catalysis, forward and reverse catalysis, and always showed the opposite catalytic effect in sulfite- and sulfate-fueled Sammox-driven CRNs, respectively, at selected high and low temperatures, presenting seesaw-like catalytic properties (Fig. 5 c).

## 3.3. Relationship between Sammox-driven CRNs and proto-metabolisms

Here, we proposed that the peptides generated from sulfite-fueled Sammox-driven CRNs should catalyze the key reactions, such as sulfite-fueled Sammox (Fig. 1; Eq. (1)) and Anammox reactions (Fig. 1; Eq. (3)). Dissimilatory sulfite reductase (DsrAB) is closely related to the assimilatory enzyme present in all domains of life and is

Table 2
Identified selected peptides in Sammox-driven CRNs. Sulfi, peptides from sulfite-fueled CRNs; Sulfa, peptides from sulfate-fueled CRNs.

| Peptides ID | Denovo peptides | m/z | Area | Score | ppm |
|---|---|---|---|---|---|
| Sulfi-1 | NHVALAGK | 405.2346 | 9.88E + 05 | 91 | −1.1 |
| Sulfi-2 | PPLPRNN | 404.2218 | 6.79E + 05 | 80 | −13.4 |
| Sulfi-3 | P(+42.01)VLLPPLA | 431.2729 | 2.65E + 06 | 71 | −6.8 |
| Sulfi-4 | PGKELPLA | 412.7466 | 1.34E + 06 | 69 | −2 |
| Sulfi-5 | VVVAAKTPPLA | 533.3416 | 3.44E + 04 | 68 | 8.6 |
| Sulfi-6 | TLVVLPNA | 413.7555 | 2.79E + 06 | 67 | 0.5 |
| Sulfi-7 | KLVELYC(+57.02)LVVYLKKKK | 506.8149 | 1.74E + 06 | 93 | 1.9 |
| Sulfi-8 | V(+42.01)YLPL | 323.6943 | 1.55E + 05 | 66 | 0.5 |
| Sulfi-9 | GPDKST | 604.3033 | 1.47E + 06 | 65 | 16 |
| Sulfi-10 | PPPLTTLA | 405.242 | 8.51E + 05 | 65 | 0 |
| Sulfa-1 | AAVLEKLE | 436.7605 | 5.53E + 06 | 99 | 5.7 |
| Sulfa-2 | DVLLSK | 337.7093 | 7.34E + 07 | 99 | 4.6 |
| Sulfa-3 | GHEVTLEALPK | 597.3336 | 4.69E + 07 | 99 | 6.1 |
| Sulfa-4 | LAEGALDKGHEVTL | 726.8925 | 5.69E + 07 | 99 | 5.8 |
| Sulfa-5 | LALEGAL | 686.4097 | 3.10E + 06 | 99 | 2.1 |
| Sulfa-6 | VATVSLPR | 421.7609 | 3.09E + 07 | 98 | 6.1 |
| Sulfa-7 | LLSSLGDEE | 962.4675 | 2.32E + 06 | 99 | −0.1 |
| Sulfa-8 | LTLTE | 576.3276 | 5.60E + 07 | 99 | 6.3 |
| Sulfa-9 | LSSLGDEE | 849.3886 | 2.04E + 07 | 99 | 6 |
| Sulfa-10 | TATKTC(+57.02)DATKT | 599.2965 | 1.82E + 08 | 73 | 6.4 |

an enzyme of primordial origin (Wagner et al., 1998; Grein et al., 2013). Because the functional divergence of assimilatory and dissimilatory sulfite reductases preceded the separation of the bacterial and archaeal domains (Crane et al., 1995; Molitor et al., 1998; Dhillon et al., 2005), LUCA most likely had a primordial sulfite reductase. Sulfite respiration required sulfite, formate, or hydrogen all of which were present in the Sammox-driven CRNs (Figs. 1, 2), implying the feasible emergence of sulfite reductase from Sammox-driven CRNs. Sulfite reductases from some sources can catalyze the reduction of both sulfite and nitrite (Crane and Getzoff, 1996), acting as nitrite reductase. As a result, the peptides generated from sulfite-fueled Sammox-driven CRNs may also catalyze Anammox reaction, as nitrite reductase (Nir) is a key enzyme in Anammox reaction (Strous et al., 2006).

In experiments described in part 2.5, results demonstrated that peptides that were generated from sulfite-fueled Sammox reaction solutions, could facilitate the consumption of sulfite and ammonium in sulfite-fueled Sammox-driven CRNs (Fig. 9 a, b). More sulfate was generated through the sulfur redox cycle (Fig. 8) in the peptides amendment group (Fig. 9 a). We also detected a trace of thiosulfate, as it was reported that thiosulfate can be generated through the sulfur redox cycle (He et al., 2019). Peptides that were generated from sulfite-fueled Sammox reaction solutions could facilitate the consumption of nitrite and ammonium in the Anammox reaction (Fig. 9 c).

## 4. DISCUSSION

### 4.1. Peptides formation in Sammox-driven CRNs

Sulfide is an essential reductant in abiotic $CO_2$ reduction to organics (Wang et al., 2013). The first observation of $CO_2$ reduction to formate with $H_2S$ in a simulated hydrothermal vent system was reported by He et al. (He et al., 2019) (Fig. 1; Eqs. (5), (6); x = 3 or 4). During this reaction, over 80% $S^{2-}$ was oxidized to $SO_3^{2-}$ and others to $SO_4^{2-}$ (Eq. (5)). The sulfur redox cycle can be obtained through $SO_3^{2-}/SO_4^{2-}$ reduction to $S^{2-}$ by organic carbon (Wang et al., 2013; He et al., 2019). In this study, the sulfur redox cycle can be obtained through $SO_3^{2-}/SO_4^{2-}$ reduction to $S^{2-}$ by $NH_4^+$, the Sammox process (Fig. 8). In a different manner, $NH_4^+$ could preserve the organic compounds in Sammox-driven CRNs. Water-gas shift reaction occurred in Sammox-driven CRNs, resulting in the production of active $H_2$ and CO (Eqs. (7), (8), (9)) (Balcerowiak, 1985; Li et al., 2020b). Active $H_2$ was employed to reduce $CO_2$, and α-keto acids production (Fig. 8). Formate may react with ammonium to produce ammonium formate (Fig. 1; Eq. (10)) (Wu et al., 2020). Ammonium formate may be both hydrogen and nitrogen sources for the reductive amination of α-keto acids (Wu et al., 2020). Ammonium formate reacted with pyruvate, oxaloacetate, and α-ketoglutarate to produce alanine, glycine, leucine, serine, glutamate, and aspartate. That is because heating ammonium formate turns it into formamide (Fig. 1; Eq. (11)), which acts as a chemical precursor for pyruvate, oxaloacetate, and α-ketoglutarate production (Saladino et al., 2012). Succinate, malate, and fumarate can be generated from oxaloacetate, by a reductive dehydroxylation step to yield succinate, and a two-electron–two-proton reduction step to yield malate, a β-elimination of $H_2O$ to yield fumarate, whereas α-ketoglutarate can be produced by adding a one-carbon unit to succinate (Saladino et al., 2012). Other possible pathways, such as carboxylic acids and amino acids, which could be the products of sodium cyanide and ammonium chloride at 38 °C cannot be ruled out (Ruiz-Bermejo et al., 2012). Because heating of formamide at higher temperatures will produce hydrogen cyanide, and this condition can be met in our experiment (Eq. (12)).
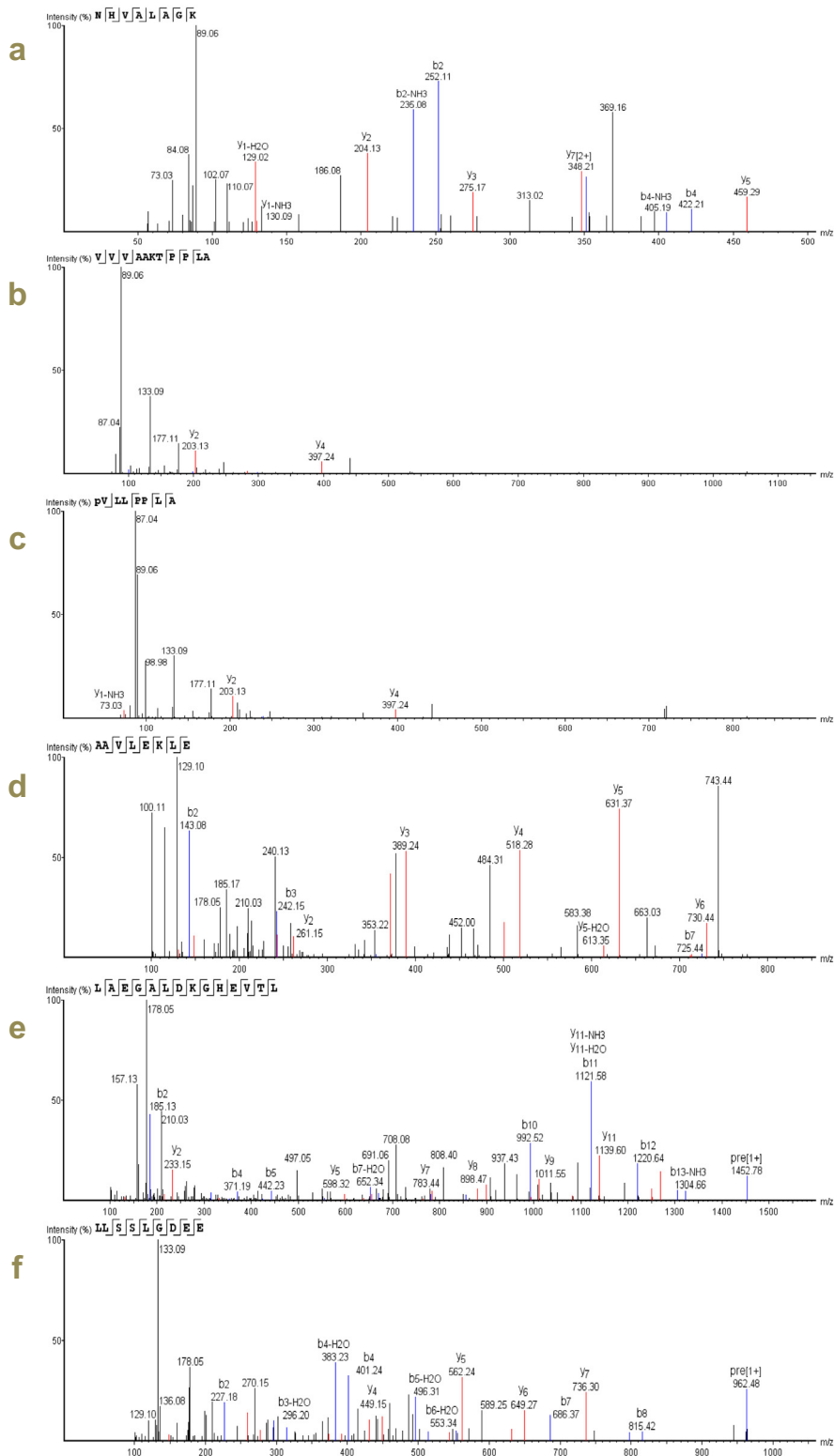
$$HCONH_2 \rightarrow HCN + H_2O \qquad (12)$$

Fig. 4. MS/MS spectra of Sammox-driven CRNs-generated peptides. All experiences were conducted in positive electrospray ionization mode. The spectra of selected three peptides a–c were from sulfite-fueled Sammox-driven CRNs. The spectra of selected three peptides d–f were from sulfate-fueled Sammox-driven CRNs. The left side of all peptides sequences in the figure is N-terminal and the right side is C-terminal.
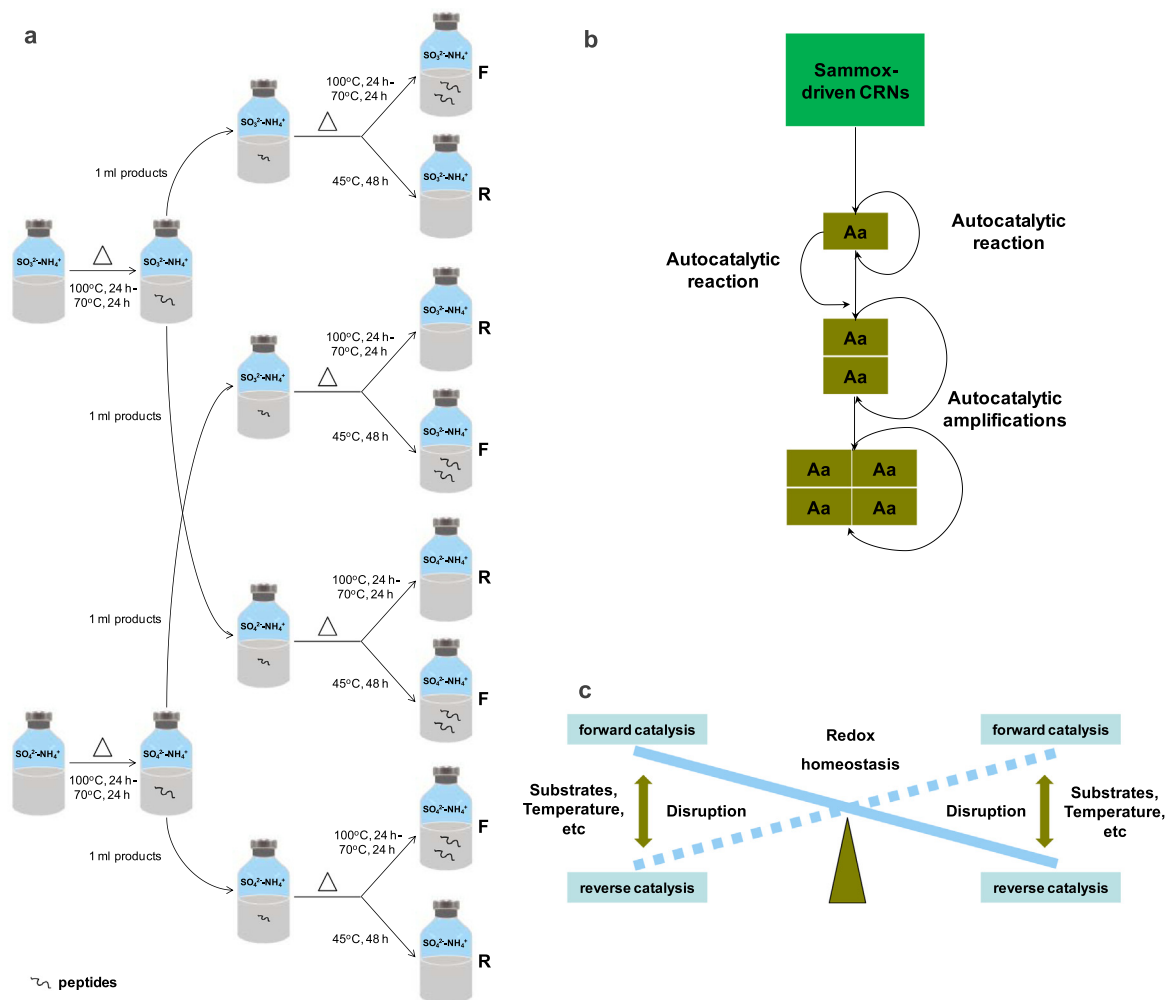
Fig. 5. Diagram of detection of autocatalysis in Sammox-driven CRNs. A, experimental procedure and results summary (F: forward catalysis, R: reverse catalysis). B, expected autocatalytic amplification of peptides in the Sammox-driven CRNs (Aa: amino acid). C, Seesaw-like catalytic impacts of peptides on the redox homeostasis of Sammox-driven CRNs due to the variation of temperature and substrates concentration.

There is no peptides production or low concentration of peptides production in sulfide-fueled CRNs, which may require higher reaction temperature and/or accelerators. It is worth mentioning that sulfite should be accelerator during reductive amination (Wang et al., 2012; Xu et al., 2018). Sulfite-fueled CRNs may be viable Sammox-driven CRNs that contribute to the production of peptides under mild primordial conditions, as sulfate would have been severely limited in the primordial environment (Canfield et al., 2006; Crowe et al., 2014; Moore et al., 2017; Colman et al., 2020).

We have not found free proteinogenic amino acids or the content is very low in Sammox-driven CRNs. This indicates that the Sammox-driven CRNs facilitate amino acids polymerization, given that carbon disulfide ($CS_2$) and carbonyl sulfide (COS), components of the interaction of hydrogen sulfide and carbon dioxide under mild circumstances in an anaerobic aqueous environment (Heinen and Lauwers, 1996), could promote peptide bond formation (Leman et al., 2004, 2015; Frenkel-Pinter et al.,

2020). It should be noted that we can only identify peptides of 4–30 amino acids by nano LC-MS/MS in this study. We then cannot identify other types of peptides that might exist, such as dipeptides. In addition, other organics are likely to be produced in Sammox-driven CRNs, in view of the prebiotic formamide can lead to chemical precursor for nucleic bases, biogenic carboxylic acids, sugars, amino sugars, amino acids synthesis (Saladino et al., 2012).

In this study, the 15 proteinogenic amino acids required only a few steps in their metabolism from the incomplete rTCA (Hartman 1975). Alanine, glycine, valine, leucine, serine, and cysteine are closely linked to pyruvate. Aspartate, asparagine, lysine, tyrosine and threonine are linked to oxaloacetate. Glutamate, proline, and arginine are linked to α-ketoglutarate. Notably, compared to other amino acids, the frequency of the most ancient amino acids—glycine, alanine, aspartate, and glutamate—was relatively high compared to other amino acids (Table 1), which can be explained by existing theories (Wong, 2005; Trifonov et al., 2012). The frequency of serine was also relatively
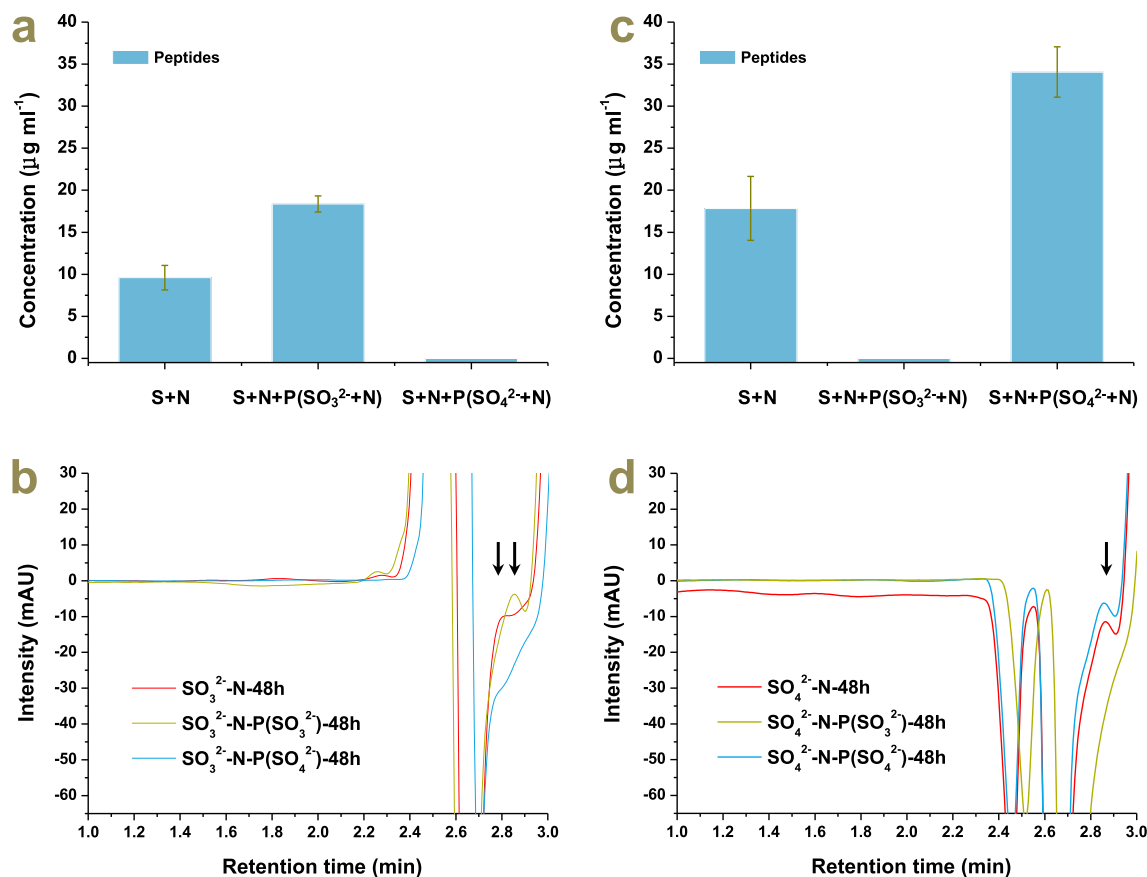
Fig. 6. Autocatalysis of the Sammox-driven CRNs under 100 °C–70 °C after 48 h reaction (a, peptides in sulfite-fueled CRNs; c, peptides in sulfate-fueled CRNs). The detection was performed at 214 nm. For a and c, treatments were as follows from left to right: sulfurous species with ammonium; sulfurous species with ammonium plus 1.0 mL products from sulfite-fueled CRNs; sulfurous species with ammonium plus 1.0 mL products from sulfate-fueled CRNs. Chromatogram of peptides generated from Sammox-driven CRNs (b, sulfite-fueled CRNs; d, sulfate-fueled CRNs). For b and d, the red color line indicates the treatment group of sulfurous species with ammonium; olive color line indicates treatment group of sulfurous species with ammonium plus 1.0 mL products from sulfite-fueled CRNs; blue color line indicates treatment group of sulfurous species with ammonium plus 1.0 mL products from sulfate-fueled CRNs. The arrows demonstrate the peaks of peptides. Error bars illustrate standard deviations of three replicates ($P < 0.05$).

high, as it is conserved in ancestral ferredoxin (Eck and Dayhoff, 1966). More importantly, the frequency of glycine, alanine, aspartate, glutamate, and serine as conserved amino acids is in accordance with the earliest stage of genetic code evolution (Davis, 2002).

### 4.2. Disruption regulated switchable bidirectional catalysis in Sammox-driven prebiotic CRNs

Primordial peptides that synthesized by Sammox-driven CRNs should be multifunctional peptides with low substrate specificity; hence, they should be connected mechanistically and evolutionarily. It has been proposed that any sufficiently complex set of polypeptides will inevitably generate reflexively autocatalytic sets of peptides and polypeptides (Kauffman, 1986). In 1996, Lee et al. demonstrated that a rationally designed 32-residue α-helical peptide could act autocatalytically in templating its own synthesis by accelerating thioester-promoted amide-bond condensation in neutral aqueous solutions, indicating that the peptide has the possibility of self-replication (Lee

et al., 1996). Other studies have proposed that not only do some dipeptides and short peptides have catalytic activities, but even a single proline can have aldolase activity (Sakthivel et al., 2001; Jarvo and Miller, 2002). In this study, the catalytic direction of peptides was switchable owing to temperature variation and/or the ratio of sulfite to sulfate, keeping Sammox-driven CRNs with both anabolic and catabolic reactions at all times. As enzymes are intrinsically bidirectional, a newly evolved enzyme can not be assigned to either autotrophic or heterotrophic metabolism. Enzymes that were able to catalyze the synthesis of $CO_2$ to organic macromolecules were principally able to catalyze the degradation of the respective products as well (Gutekunst, 2018). As is well known that redox homeostasis is a fundamental property of life, which is a set of enzyme-assisted metabolic reactions to maintain life. How this homeostatic system evolved and functioned before the emergence of enzyme networks is an extremely important challenge in exploring the origin of life. The results presented in this study show that Sammox-driven CRNs may possesses such characteristics. The variation of substrates
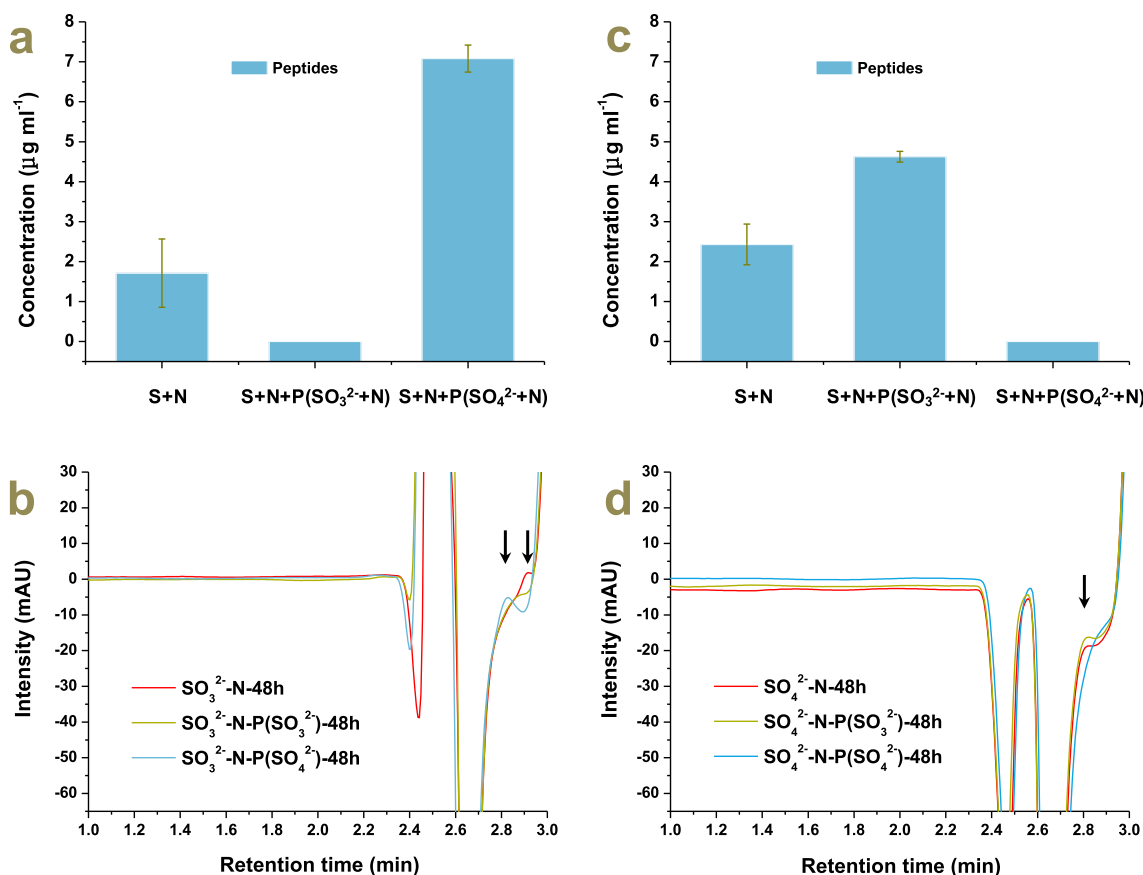
Fig. 7. Autocatalysis of the Sammox-driven CRNs under 45 °C after 48 h reaction (a, peptides in sulfite-fueled CRNs; c, peptides in sulfate-fueled CRNs). The detection was performed at 214 nm. For a and c, treatments were as follows from left to right: sulfurous species with ammonium; sulfurous species with ammonium plus 1.0 mL products from sulfite-fueled CRNs; sulfurous species with ammonium plus 1.0 mL products from sulfate-fueled CRNs. Chromatogram of peptides generated from Sammox-driven CRNs (b, sulfite-fueled CRNs; d, sulfate-fueled CRNs). For b and d, the red color line indicates the treatment group of sulfurous species with ammonium; olive color line indicates treatment group of sulfurous species with ammonium plus 1.0 mL products from sulfite-fueled CRNs; blue color line indicates treatment group of sulfurous species with ammonium plus 1.0 mL products from sulfate-fueled CRNs. The arrows demonstrate the peaks of peptides. Error bars illustrate standard deviations of three replicates (P < 0.05).

concentration, such as sulfur, ammonium, bicarbonate may disrupt the redox homeostasis of Sammox-driven CRNs, therefore, the catalytic orientation of peptides changed due to the stimulation, to maintain redox homeostasis of the whole system, similar to the $FeS/S/FeS_2$ redox system (Wang et al., 2011). In this sense, any factor that can influence the redox property of the system, will disrupt the redox homeostasis, consequently may cause a change in the direction of peptides catalysis, for instance, temperature and pH. So far, we do not know the exact intrinsic mechanisms of seesaw-like catalytic impacts, but it is critical to achieving the sustainability and evolution of Sammox-driven CRNs.

Some of the peptides generated in the Sammox-driven CRNs would undoubtedly function as proto-proteases, which cleave unstructured peptides more rapidly than structured ones, and also since functional peptides must have some degree of structure, the proto-proteases would preferentially destroy non-functional peptides (New and Pohorille, 2000). Ornithine, a basic amino acid that presents in primordial proteins yet is absent in modern-day proteins. Notably, guanidination of ornithine in primordial peptides

to give arginine can be performed chemically by simple reagents such as cyanamide (Alonso-Moreno et al., 2014), hence, promotes proto-proteins folding and functionalization (Longo et al., 2020). And occasionally, the newly produced peptides would be capable of performing high substrate specificities and/or novel functions. The catalytic capabilities of the Sammox-driven CRNs as a whole can thus increase due to more and more peptides with high substrate specificities and/or novel functions are selectively survived.

### 4.3. From Sammox-driven CRNs to proto-metabolisms

In another sense, this result suggests a common origin of evolutionary metabolism and catabolism since sulfite and sulfate were consistently co-occurring in the Sammox-driven CRNs through the sulfur redox cycle (Fig. 8). The Sammox-driven CRNs might be PMNs of both autotrophy and heterotrophy. As a result, there may be multiple types of metabolisms stemming from the Sammox-driven CRNs. For example, Sammox, Anammox, formate/hydrogen oxi-
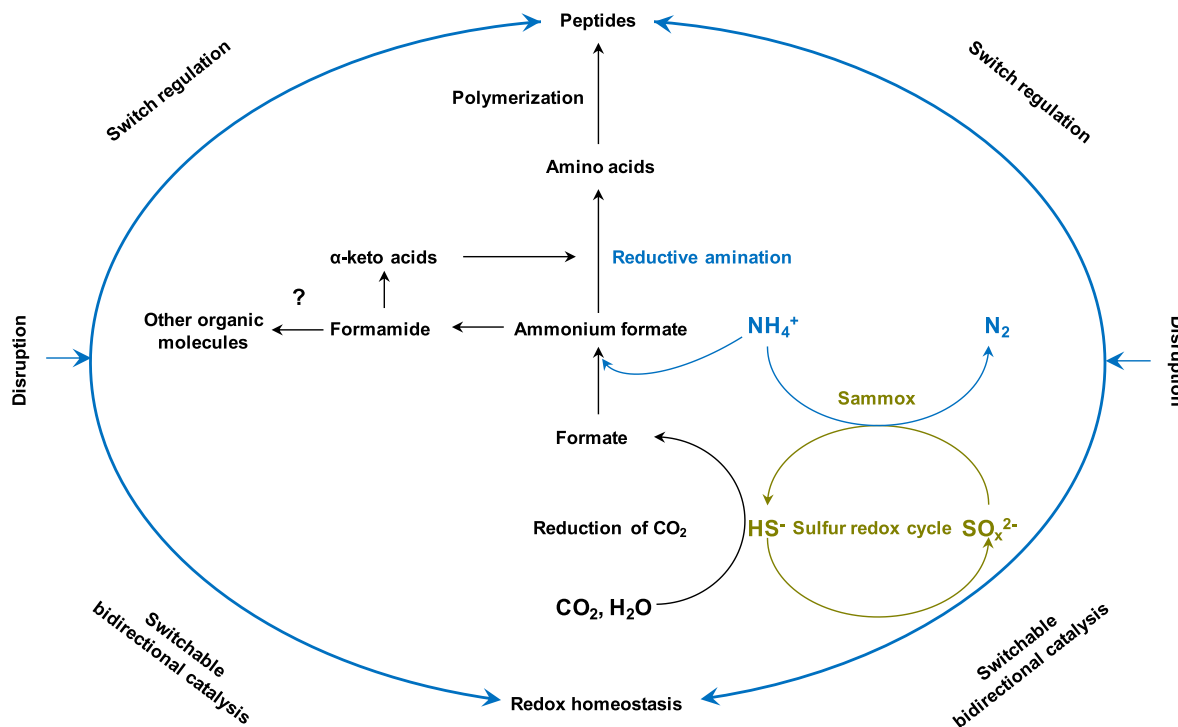
Fig. 8. Demonstrates the conceptual model of Sammox-driven coupled transformation of carbon, hydrogen, oxygen, nitrogen, sulfur simultaneously in nonequilibrium thermodynamic environments, initiating the emergence of prebiotic autocatalytic CRNs. Switchable bidirectional catalysis of peptides was regulated by disruption of redox homeostasis in Sammox-driven prebiotic CRNs. x = 3, 4.

dation coupled with dissimilatory sulfite reduction, dissimilatory nitrite reduction to ammonium (nitrite ammonification), or peptides/protein degradation. If Sammox-driven CRNs could have driven the emergence of LUCA, the direct descendant of LUCA should have similar energy conservation pathways as Sammox-driven CRNs. Accordingly, Planctomycetes could be the first emerging bacterial group, based on analysis of the bacterial phylogeny through rRNA sequences (Brochier and Philippe, 2002). It is also declared that Planctomycetes might be transitional forms between the three domains of life (Reynaud and Devos, 2011), implying a planctobacterial origin of Nomura (eukaryotes, archaea) (Cavalier-Smith and Chao, 2020). The planctomycete *Gemmata obscuriglobus* was the only microorganism capable of protein endocytosis and degradation, implying

an intermediate stage between bacteria and eukaryotes (Lonhienne et al., 2010; Acehan et al., 2014). On the other hand, all Anammox microorganisms belong to a monophyletic group, deepest branching inside the phylum Planctomycetes (van Niftrik and Jetten, 2012), and is the only microorganism with membranes comprising both ether-linked lipids (found in archaeal lipids) and ester-linked lipids (found in bacterial and eukaryotic lipids), suggesting a plausible intermediate for the development of the archaeal membrane (Devos and Reynaud, 2010). Therefore, Anammox microorganisms might be the predominant primordial species in Planctomycetes.

A recent study demonstrated the mixotrophic feather of Anammox microorganisms *Candidatus* "*Kuenenia stuttgartiensis*" directly assimilates extracellular formate through
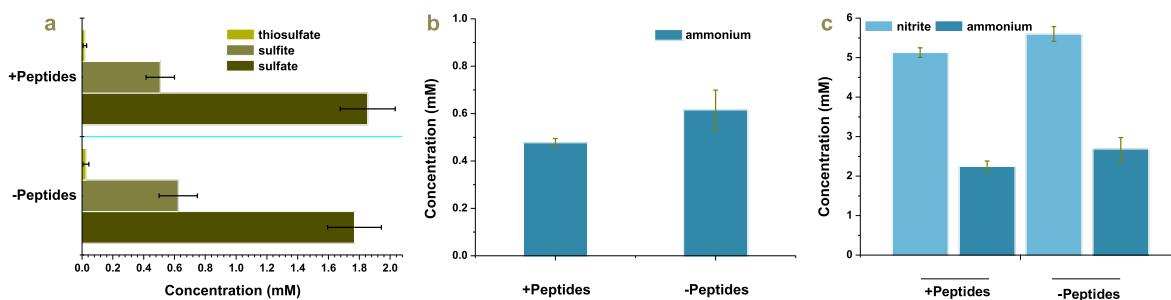


Fig. 9. Peptides that were generated from sulfite-fueled Sammox reaction solutions, facilitated the consumption of sulfite and ammonium in sulfite-fueled Sammox-driven CRNs, and nitrite and ammonium in Anammox reaction. Data are all obtained after 48 h of reaction. Error bars indicate standard deviations of three replicates.

the Wood–Ljungdahl pathway instead of oxidizing it completely to $CO_2$ (Lawson et al., 2021). Experimental investigation together with genomic evidence has also inferred that Anammox microorganisms can perform reverse metabolism of Anammox, which utilize alternative electron donors to ammonium, such as formate, acetate, and propionate for energy conservation with nitrite or nitrate as electron acceptors (Güven et al., 2005; Strous et al., 2006; Kartal et al., 2007; Lawson et al., 2021). The proto-metabolisms that may allow LUCA to absorb electrons from carbohydrate oxidation and provide a reductant for $CO_2$ fixation could have evolved in two connected organisms or a single cell (Gutekunst, 2018). A pure culture of Anammox microorganisms is yet to be discovered (Kuenen, 2020), implying that Anammox microorganisms may require symbiont to survive. The unique characteristics of Planctomycetes are consistent with the inferences for proto-metabolism, and Anammox microorganisms may be the direct descendant of Sammox-driven CRNs. The functional microorganisms were majorly Anammox microorganisms or Planctomycetes in sulfate-dependent ammonium oxidation environment (Liu et al., 2021), suggesting that the Sammox-driven CRNs can support primordial Anammox metabolism. Indeed, nitrite reduction coupled with ammonium oxidation occurred in Sammox-driven CRNs (Fig. 1; Eq. (3)). Our findings infer an intrinsic relationship between Sammox-driven CRNs and proto-metabolisms, and the common evolutionary origin of Sammox and Anammox. Sammox and Anammox are primordial energy conservation traits.

### 4.4. Implications

The ideas presented in our study show their own logical self-consistency and compatibility with the merits of other existing theories. Our findings hint that the PMNs would necessarily rise from coupling transformation of C, H, O, N, and S at their earliest stage of the transition from geochemistry to biochemistry under mild hydrothermal conditions. The co-evolution of five key elements metabolism might be strong explanation for life origin and why the structure of metabolic networks is as it is. Sulfurous species and ammonium are all indispensable for the construction of Sammox-driven PMNs. Therefore, our study explained why sulfur reduction and anaerobic ammonia oxidation are the primordial types of metabolism.

Redox homeostasis may evolve from the transition from Sammox-driven CRNs to Sammox-driven PMNs after autocatalytic peptides formation. The catalysis of peptides in Sammox-driven PMNs is bidirectional, and switchable when system is disturbed, such as variation of substrates and temperature, thus exhibit both anabolic and anabolic characteristics. The seesaw-like catalytic characteristics of peptides make it possible to evolve, and achieving the sustainability and evolution of Sammox-driven PMNs. In addition, our findings support the synchronistic evolution of autotrophy and heterotrophy.

This research may also shed light on the exploration of extraterrestrial life. We should be especially concerned the hotspots where Sammox-driven CRNs can be maintained.

The exploration of Sammox-driven CRNs opened up a new perspective for the understanding of the emergence of biochemistry from geochemistry. Several questions naturally arise. Such as geological adaptation range of Sammox-driven CRNs, from mild hydrothermal to freeze–thaw condition, from anaerobic to microaerobic condition, from redox-initiated to photoinitiated reactions. Can phosphorous-dependent Sammox-driven CRNs find merit of RNA world theory? How long will it take to produce proto-cells from phosphorous-dependent Sammox-driven CRNs? Whether there is pre-Darwinian evolution in Sammox-driven CRNs?

## 5. CONCLUSIONS

This study reports that the simplest substances—$CO_2$, sulfite/sulfate, and ammonium—were converted to peptides in one geological setting by Sammox-driven CRNs which consisted of $CO_2$ fixation and reductive amination. Peptides, with 15 proteinogenic amino acids, provide the Sammox-driven CRNs with autocatalysis. Peptides exhibit bidirectional catalysis, with the opposite catalytic effect in sulfite and sulfate-fueled Sammox-driven CRNs, respectively, at both a variable temperature range and a fixed temperature, resulting in seesaw-like catalytic characteristics. Factors that can influence the redox property of the Sammox-driven CRNs, will disrupt the redox homeostasis, may consequently cause a change in the direction of peptides catalysis. The seesaw-like catalytic characteristics of peptides enable Sammox-driven CRNs to maintain both anabolic and catabolic reactions at all times. This result suggests a common origin of primordial metabolism and catabolism since sulfite and sulfate were co-occurring consistently in the Sammox-driven CRNs through the sulfur redox cycle. In addition, peptides generated from sulfite-fueled Sammox-driven CRNs can catalyze both sulfite-fueled Sammox and Anammox reactions. Combining the unique characteristics of Anammox microorganisms with the inference of proto-metabolism, Sammox and Anammox are primordial energy conservation traits. We infer that Sammox-driven CRNs, under mild conditions, are critical for driving the origin of life.

### Declaration of Competing Interest

The authors declare that they have no known competing financial interests or personal relationships that could have appeared to influence the work reported in this paper.

Xian-Ming Bao (鲍显明) for his kind encouragement and support.

## AUTHOR CONTRIBUTIONS

## APPENDIX A. SUPPLEMENTARY DATA

Supplementary data associated with this article including Figs. S1–S11 can be found online at https://doi.org/10.1016/j.gca.2022.03.004.

## REFERENCES

Acehan D., Santarella-Mellwig R. and Devos D. P. (2014) A bacterial tubulovesicular network. *J. Cell. Sci.* **127**(2), 277–280.

Alonso-Moreno C., Antiñolo A., Carrillo-Hermosilla F. and Otero A. (2014) Guanidines: from classical approaches to efficient catalytic syntheses. *Chem. Soc. Rev.* **43**(10), 3406–3425.

Amend J. P. and Shock E. L. (2001) Energetics of overall metabolic reactions of thermophilic and hyperthermophilic Archaea and Bacteria. *FEMS Microbiol. Rev.* **25**(2), 175–243.

Amend J. P., Rogers K. L., Shock E. L., Gurrieri S. and Inguaggiato S. (2003) Energetics of chemolithoautotrophy in the hydrothermal system of Vulcano Island, southern Italy. *Geobiology* **1**(1), 37–58.

Anbar A. D. (2008) Oceans. Elements and evolution. *Science* **322**(5907), 1481–1483.

Balcerowiak W. (1985) The thermal decomposition of HCOONa in presence of NaOH. *Thermochim. Acta* **92**, 661–663.

Brochier C. and Philippe H. (2002) Phylogeny: a non-hyperther-mophilic ancestor for bacteria. *Nature* **417**(6886), 244.

Canfield D. E., Rosing M. T. and Bjerrum C. (2006) Early anaerobic metabolisms. *Phil. Trans. R. Soc. B* **361**(1474), 1819–1834.

Cavalier-Smith T. and Chao E. E. Y. (2020) Multidomain ribosomal protein trees and the planctobacterial origin of neomura (eukaryotes, archaebacteria). *Protoplasma* **257**(3), 621–753.

Colman D. R., Lindsay M. R., Amenabar M. J., Fernandes-Martins M. C., Roden E. R. and Boyd E. S. (2020) Phyloge-nomic analysis of novel Diaforarchaea is consistent with sulfite but not sulfate reduction in volcanic environments on early Earth. *ISME J.* **14**(5), 1316–1331.

Crane B. R. and Getzoff E. D. (1996) The relationship between structure and function for the sulfite reductases. *Curr. Opin. Struct. Biol.* **6**(6), 744–756.

Crane B. R., Siegel L. M. and Getzoff E. D. (1995) Sulfite reductase structure at 1.6 angstrom—evolution and catalysis for reduction of inorganic anions. *Science* **270**(5233), 59–67.

Crowe S. A., Paris G., Katsev S., Jones C., Kim S. T., Zerkle A. L., Nomosatryo S., Fowle D. A., Adkins J. F., Sessions A. L., Farquhar J. and Canfield D. E. (2014) Sulfate was a trace constituent of Archean seawater. *Science* **346**(6210), 735–739.

Davis B. K. (2002) Molecular evolution before the origin of species. *Prog. Biophys. Mol. Biol.* **79**(1–3), 77–133.

Devos D. P. and Reynaud E. G. (2010) Intermediate steps. *Science* **330**(6008), 1187–1188.

Dhillon A., Goswami S., Riley M., Teske A. and Sogin M. (2005) Domain evolution and functional diversification of sulfite reductases. *Astrobiology* **5**(1), 18–29.

Eck R. V. and Dayhoff M. O. (1966) Evolution of the structure of ferredoxin based on living relics of primitive amino acid sequences. *Science* **152**(3720), 363–366.

Falkowski P. G., Fenchel T. and Delong E. F. (2008) The microbial engines that drive Earth's biogeochemical cycles. *Science* **320**(5879), 1034–1039.

Fdz-Polanco F., Fdz-Polanco M., Fernandez N., Uruena M. A., Garcia P. A. and Villaverde S. (2001) Combining the biological nitrogen and sulfur cycles in anaerobic conditions. *Water Sci. Technol.* **44**(8), 77–84.

Frenkel-Pinter M., Samanta M., Ashkenasy G. and Leman L. J. (2020) Prebiotic peptides: Molecular hubs in the origin of life. *Chem. Rev.* **120**(11), 4707–4765.

Grein F., Ramos A. R., Venceslau S. S. and Pereira I. A. C. (1827) (2013) Unifying Concepts in anaerobic respiration: Insights from dissimilatory sulfur metabolism. *BBA-Bioenerg.* **2**, 145–160.

Gutekunst K. (2018) Hypothesis on the synchronistic evolution of autotrophy and heterotrophy. *Trends Biochem. Sci.* **43**(6), 402–411.

Güven D., Dapena A., Kartal B., Schmid M. C., Maas B., van de Pas-Schoonen K., Sozen S., Mendez R., Op den Camp H. J. M., Jetten M. S. M., Strous M. and Schmidt I. (2005) Propionate oxidation by and methanol inhibition of anaerobic ammonium-oxidizing bacteria. *Appl. Environ. Microbiol.* **71**(2), 1066–1071.

Hartman H. (1975) Speculations on the origin and evolution of metabolism. *J. Mol. Evol.* **4**(4), 359–370.

He R. T., Hu B. Y., Zhong H., Jin F. M., Fan J. J., Hu Y. H. and Jing Z. Z. (2019) Reduction of $CO_2$ with $H_2S$ in a simulated deep-sea hydrothermal vent system. *Chem. Commun.* **55**(8), 1056–1059.

Heinen W. and Lauwers A. M. (1996) Organic sulfur compounds resulting from the interaction of iron sulfide, hydrogen sulfide and carbon dioxide in an anaerobic aqueous environment. *Orig. Life Evol. Biosph.* **26**(2), 131–150.

Hordijk W., Steel M. and Dittrich P. (2018) Autocatalytic sets and chemical organizations: modeling self-sustaining reaction net-works at the origin of life. *New J. Phys.* **20** 015011.

Jarvo E. R. and Miller S. J. (2002) Amino acids and peptides as asymmetric organocatalysts. *Tetrahedron* **58**(13), 2481–2495.

Kartal B., Kuypers M. M. M., Lavik G., Schalk J., den Camp H. J. M. O., Jetten M. S. M. and Strous M. (2007) Anammox bacteria disguised as denitrifiers: nitrate reduction to dinitrogen gas via nitrite and ammonium. *Environ. Microbiol.* **9**(3), 635–642.

Kauffman S. A. (1986) Autocatalytic sets of proteins. *J. Theor. Biol.* **119**(1), 1–24.

Kuenen J. G. (2020) Anammox and beyond. *Environ. Microbiol.* **22**(2), 525–536.

Lawson C. E., Nuijten G. H. L., de Graaf R. M., Jacobson T. B., Pabst M., Stevenson D. M., Jetten M. S. M., Noguera D. R., McMahon K. D., Amador-Noguez D. and Lücker S. (2021) Autotrophic and mixotrophic metabolism of an anammox bacterium revealed by in vivo $^{13}$C and $^{2}$H metabolic network mapping. *ISME J.* **15**(3), 673–687.

Lee D. H., Granja J. R., Martinez J. A., Severin K. and Ghadiri M. R. (1996) A self-replicating peptide. *Nature* **382**(6591), 525–528.

Leman L., Orgel L. and Ghadiri M. R. (2004) Carbonyl sulfide-mediated prebiotic formation of peptides. *Science* **306**(5694), 283–286.

Leman L. J., Huang Z. Z. and Ghadiri M. R. (2015) Peptide bond formation in water mediated by carbon disulfide. *Astrobiology* **15**(9), 709–716.

Li G. X., Li H., Xiao K. Q. and Bao P. (2020a) Thiosulfate reduction coupled with anaerobic ammonium oxidation by *Ralstonia* sp. GX3-BWBA. *ACS Earth Space Chem.* **4**(12), 2426–2434.

Li H., Wu S. Y., Wu Y. Q., Huang S. and Gao J. S. (2020b) Process characteristics and mechanism of $Na_2CO_3$-catalyzed water-gas shift reaction in a benzene-containing hydrothermal system. *Fuel* **275** 117917.

Li Y. and Keppler H. (2014) Nitrogen speciation in mantle and crustal fluids. *Geochim. Cosmochim. Acta* **129**, 13–32.

Liu L. Y., Xie G. J., Xing D. F., Liu B. F., Ding J., Cao G. L. and Ren N. Q. (2021) Sulfate dependent ammonium oxidation: A microbial process linked nitrogen with sulfur cycle and potential application. *Environ. Res.* **192** 110282.

Longo L. M., Despotovic D., Weil-Ktorza O., Walker M. J., Jabłonska J., Fridmann-Sirkis Y., Varani G., Metanis N. and Tawfik D. S. (2020) Primordial emergence of a nucleic acid binding protein via phase separation and statistical ornithine-to-arginine conversion. *Proc. Natl. Acad. Sci. U. S. A.* **117**(27), 15731–15739.

Lonhienne T. G., Sagulenko E., Webb R. I., Lee K. C., Franke J., Devos D. P., Nouwens A., Carroll B. J. and Fuerst J. A. (2010) Endocytosis-like protein uptake in the bacterium *Gemmata obscuriglobus. Proc. Natl. Acad. Sci. U. S. A.* **107**(29), 12883–12888.

Mikhail S. and Sverjensky D. A. (2014) Nitrogen speciation in upper mantle fluids and the origin of Earth's nitrogen-rich atmosphere. *Nat. Geosci.* **7**(11), 816–819.

Molitor M., Dahl C., Molitor I., Schafer U., Speich N., Huber R., Deutzmann R. and Truper H. G. (1998) A dissimilatory sirohaem-sulfite-reductase-type protein from the hyperthermophilic archaeon *Pyrobaculum islandicum. Microbiology* **144** (pt 2), 529–541.

Moore E. K., Jelen B. I., Giovannelli D., Raanan H. and Falkowski P. G. (2017) Metal availability and the expanding network of microbial metabolisms in the Archaean eon. *Nat. Geosci.* **10**(9), 629–636.

New M. H. and Pohorille A. (2000) An inherited efficiencies model of non-genomic evolution. *Simul. Pract. Theory.* **8**, 99–108.

Ono S., Eigenbrode J. L., Pavlov A. A., Kharecha P., Rumble D., Kasting J. F. and Freeman K. H. (2003) New insights into Archean sulfur cycle from mass-independent sulfur isotope records from the Hamersley basin, Australia. *Earth Planet. Sci. Lett.* **213**(1–2), 15–30.

Reynaud E. G. and Devos D. P. (2011) Transitional forms between the three domains of life and evolutionary implications. *Proc. Biol. Sci.* **278**(1723), 3321–3328.

Ruiz-Bermejo M., de la Fuente J. L., Rogero C., Menor-Salvan C., Osuna-Esteban S. and Martín-Gago J. A. (2012) New insights into the characterization of 'insoluble black HCN polymers'. *Chem. Biodivers.* **9**(1), 25–40.

Sakthivel K., Notz W., Bui T. and Barbas C. F. (2001) Amino acid catalyzed direct asymmetric aldol reactions: A bioorganic approach to catalytic asymmetric carbon-carbon bond-forming reactions. *J. Am. Chem. Soc.* **123**(22), 5260–5267.

Saladino R., Botta G., Pino S., Costanzo G. and Di Mauro E. (2012) Genetics first or metabolism first? The formamide clue. *Chem. Soc. Rev.* **41**(16), 5526–5565.

Schrum H. N., Spivack A. J., Kastner M. and D'Hondt S. (2009) Sulfate-reducing ammonium oxidation: A thermodynamically feasible metabolic pathway in subseafloor sediment. *Geology* **37** (10), 939–942.

Strous M., Pelletier E., Mangenot S., Rattei T., Lehner A., Taylor M. W., Horn M., Daims H., Bartol-Mavel D., Wincker P., Barbe V., Fonknechten N., Vallenet D., Segurens B., Schenowitz-Truong C., Medigue C., Collingro A., Snel B., Dutilh B. E., Op den Camp H. J. M., van der Drift C., Cirpus I., van de Pas-Schoonen K. T., Harhangi H. R., van Niftrik L., Schmid M., Keltjens J., van de Vossenberg J., Kartal B., Meier H., Frishman D., Huynen M. A., Mewes H. W., Weissenbach J., Jettern M. S. M., Wagner M. and Le Paslier D. (2006) Deciphering the evolution and metabolism of an anammox bacterium from a community genome. *Nature* **440**(7085), 790–794.

Trifonov E. N., Volkovich Z. and Frenkel Z. M. (2012) Multiple levels of meaning in DNA sequences, and one more. *Ann. N Y Acad. Sci.* **1267**, 35–38.

van Niftrik L. and Jetten M. S. M. (2012) Anaerobic ammonium-oxidizing bacteria: unique microorganisms with exceptional properties. *Microbiol. Mol. Biol. Rev.* **76**(3), 585–596.

Wagner M., Roger A. J., Flax J. L., Brusseau G. A. and Stahl D. A. (1998) Phylogeny of dissimilatory sulfite reductases supports an early origin of sulfate respiration. *J. Bacteriol.* **180**(11), 2975–2982.

Wang W., Li Q. L., Yang B., Liu X. Y., Yang Y. Q. and Su W. H. (2012) Photocatalytic reversible amination of α-keto acids on a ZnS surface: implications for the prebiotic metabolism. *Chem. Commun.* **48**(15), 2146–2148.

Wang W., Yang B., Qu Y. P., Liu X. Y. and Su W. H. (2011) FeS/S/$FeS_2$ redox system and its oxidoreductase-like chemistry in the iron-sulfur world. *Astrobiology* **11**(5), 471–476.

Wang Y. Q., Jin F. M., Zeng X., Ma C. X., Wang F. W., Yao G. D. and Jing Z. Z. (2013) Catalytic activity of Ni3S2 and effects of reactor wall in hydrogen production from water with hydrogen sulphide as a reducer under hydrothermal conditions. *Appl. Energy* **104**, 306–309.

Wong J. T. F. (2005) Coevolution theory of genetic code at age thirty. *BioEssays* **27**(4), 416–425.

Wu H. G., Yu Z. Z., Li Y., Xu Y. F., Li H. and Yang S. (2020) Hot water-promoted catalyst-free reductive cycloamination of (bio-) keto acids with $HCOONH_4$ toward cyclic amides. *J. Supercrit. Fluids* **157** 104698.

Xu J. F., Ritson D. J., Ranjan S., Todd Z. R., Sasselov D. D. and Sutherland J. D. (2018) Photochemical reductive homologation of hydrogen cyanide using sulfite and ferrocyanide. *Chem. Commun.* **54**(44), 5566–5569.

*Associate editor:* Yoko Kebukawa